Application of the Hypersonic Analogy for Validation of Numerical Simulations

Shmuel Eidelman*
Science Applications International Corporation, McLean, Virginia

This paper presents a family of self-similar solutions for hypersonic flow over a flat plate with a blunt leading edge. These solutions are derived, based on the principle of hypersonic similitude, from the solutions of the point-blast problems and include modeling of energy release (or absorption) behind the main shock front. The resulting analytical solutions are of particular interest as test problems for numerical simulations of the hypersonic flow. An example of this application is shown for hypersonic flow with $M = 32$ over a 0.025 m-thick flat plate. The numerical simulations were done using first- and second-order-accurate Godunov methods on a succession of grids covering the computational domain with increased density.

Introduction

THE design of a flight vehicle that operates at hypersonic speeds is complicated by the fact that experimental data for the regime of hypersonic flight is very limited and very expensive to obtain. Therefore, in many cases designers will rely on the results of numerical simulations of hypersonic flows. This requires powerful computers for simulation of the complicated hypersonic flows with very complex physical and chemical processes and brings to a new level importance in evaluating the accuracy of numerical simulations.

The partial differential equations describing the motion of an inviscid ideal gas (Euler equations) or viscous gas (Navier-Stokes equations) were derived under the assumption that all gas dynamics parameters and their derivatives are continuous. When these equations are solved numerically on a discrete mesh, the numerical algorithms used for solution insure a certain order of accuracy in the approximation to the differential equations. This order of accuracy can be assured reliably only for monotonic flows solved on grids with simple structures. For the more complicated cases, an accurate estimate of the numerical error is a very complex problem.

Because numerical dissipation can be studied analytically for only a very limited number of cases,[1] reliable techniques for verifying the efficiency and accuracy of numerical codes acquire special importance. Currently, there are no standard procedures or even common grounds for code testing, and authors of new codes, based on new or old methods, usually report the most successful applications. The accuracy of the numerical approximation is usually evaluated by analyzing the linearized equations, or by solving very simple test problems, which represent a very limited class of solutions. Another popular approach is to compare the results obtained with the new code with results from similar codes or with codes with a simplified mathematical formulation[2-4] (e.g., compare an Euler code with a potential code, a Navier-Stokes code with an Euler code). Frequently, Navier-Stokes solvers are compared with experimental data without noting the range of error of the experiments.

The most objective method for verification of code accuracy is to compare a numerical integration with the analytical solution of the same problem.[5] Many existing analytical solutions do not apply to practical problems in gas dynamics and, for this reason, they are not widely known. Also, their formulation is sometimes too complex. Nevertheless, such comparisons are the most accurate and unambiguous tools for studying the accuracy of numerical algorithms.

The analogy between explosion and hypersonic flow over a thin blunt body has been applied to hypersonic flow calculations.[5,6] Through the equivalence principle, t is replaced by x/U and the one-dimensional, time-dependent, self-similar problem is transformed into a two-dimensional steady-state problem. The application of similar solutions to steady flows is generally valid within the limitations discussed below. However, because some of the point-blast problems have closed-form solutions, they can be used to validate the numerical codes. In this paper, we use some recently reported solutions of the point-blast problems[7,8] to assess the accuracy of fluid dynamics codes in the hypersonic flow regime.

Problem of a Point Blast in a Reactive Medium

Basic Assumptions

Following our previous work,[7,8] we define the problem and summarize the main results for the point-blast problem in reactive medium. At time $t = 0$, a given amount of energy E_0 is released in quiescent reactive gas at the point $r = 0$ for the planar case. The cylindrical and planar cases are the most relevant for the hypersonic flow simulations. In the current study, we consider only planar symmetry. We assume that the local static pressure is negligible ($P_1 = 0$). The instantaneous energy release generates a strong shock wave, which propagates in the reactive medium and can initiate an exothermic or endothermic reaction. We look for a solution of the initial-value problem for the unsteady one-dimensional Euler equations with planar symmetry written in conservation law form:

$$\frac{\partial \rho}{\partial t} + \frac{\partial \rho U}{\partial r} = 0 \tag{1}$$

$$\frac{\partial \rho U}{\partial t} + \frac{\partial (P + \rho U^2)}{\partial r} = 0 \tag{2}$$

$$\frac{\partial e}{\partial t} + \frac{\partial (e + P)U}{\partial r} = \rho \frac{dQ}{dt} \tag{3}$$

where

$$e = \frac{P}{(\gamma - 1)} + \frac{\rho U^2}{2}$$

Received March 21, 1988; revision received Jan. 3, 1989.

*Senior Research Scientist. Member AIAA.

In Eq. (3), the right-hand term described the rate of energy release in the process of reaction. The reactive medium is assumed to be an ideal gas with a constant γ.

Under the assumptions made, namely $U_1 = 0$ and $P_1 = 0$, the conditions across the shock wave can be written as

$$U_2 = \frac{C(1+k)}{(\gamma+1)}, \quad \rho_2 = \frac{\rho_1(\gamma+1)}{(\gamma-k)}, \quad P_2 = \frac{\rho_1 C^2(1+k)}{(\gamma+1)} \tag{4}$$

where $k = [1 - (2q/C^2)(\gamma^2 - 1)]^{1/2}$, C is the shock speed, and q is the energy release at the shock wave which we will define below. Subscripts 1 and 2 indicate variables and functions ahead of and behind the shock wave front, respectively.

Solution Method

From dimensional analysis of the parameters of the problem, we conclude that for Q in the form

$$Q = \beta\left(\frac{E}{\rho_1}\right)^{n/3} t^{2n/3-2} r^{2-n} \tag{5}$$

there exists a self-similar solution to Eqs. (1-3). The value of n in Eq. (5) defines a particular self-similar solution from the group. Equation (5) is valid for planar explosions. However, it is possible to form a general solution valid for planar, cylindrical, and spherical explosions.

On the shock wave at $r = r_2$,

$$Q = q = B\left(\frac{E}{\rho_1}\right)^{n/3} t^{2n/3-2} r_2^{2-n}$$

The sign of the dimensionless parameter β determines whether energy is liberated (positive β) or absorbed (negative β) behind the shock wave.

Because our problem is self-similar, in dimensionless coordinates all parameters of the problem can be written as functions of only three nondimensional parameters γ, β, and λ, where

$$\lambda = \left(\frac{\rho_1}{E}\right)^{1/3} \frac{r}{t^{2/3}} \tag{6}$$

and E is related to the planar blast energy E_0 through a dimensionless constant $\alpha E_0 = \alpha E$.

A set of dimensionless functions, f, g, and h, depending only on λ is defined:

$$f(\lambda) = \frac{U}{U_2}, \qquad g(\lambda) = \frac{\rho}{\rho_2}, \qquad h(\lambda) = \frac{P}{P_2} \tag{7}$$

The equation of motion of the shock wave can be found from Eq. (6):

$$r_2(t) = \lambda_2\left(\frac{Et^2}{\rho_1}\right)^{1/3} \tag{8a}$$

Taking $\lambda_2 = 1$ determines that λ is changing in the interval $0 \le \lambda \le 1$ and has the value 1 on the shock wave. Thus, the equation of motion of the shock wave is

$$r_2(t) = \left(\frac{Et^2}{\rho_1}\right)^{1/3} \tag{8b}$$

and the shock speed is

$$C = \frac{2}{3}\left(\frac{E}{\rho_1 t}\right)^{1/3} \tag{9}$$

Using Eqs. (1-3), the definition of the dimensionless variables f, g, h, and the boundary conditions (4), we find a set of three first-order nonlinear equations:

$$[(1+k)f - (\gamma+1)\lambda]g' + (1+k)gf' = 0 \tag{10}$$

$$[(1+k)f - (\gamma+1)\lambda]gf' + (\gamma-k)h' - \tfrac{1}{2}(\gamma+1)fg = 0 \tag{11}$$

$$[(1+k)f - (\gamma-1)\lambda]h' + \gamma(1+k)hf' - (\gamma+1)h + M = 0 \tag{12}$$

where h', f', and g' are the derivatives of h, f, and g with respect to the argument λ. The quantities M and k are defined in the following nondimensional form:

$$k = \left[1 - \frac{9\beta}{2}(\gamma^2 - 1)\right]^{1/2} \tag{13}$$

$$M = \frac{9}{4}\beta g \frac{(\gamma+1)^3\lambda^{1-n}}{(\gamma-k)(k+1)}\left[(3-x)\lambda + (n-2)\frac{(1+k)}{(\gamma+1)}f\right] \tag{14}$$

The boundary conditions for this set of equations are $\lambda = 0$ and $f(0) = 0$ at the symmetry plane. On the shock wave, $\lambda = 1$, $f(1) = 1$, $g(1) = 1$, and $h(1) = 1$.

The total energy of the gas behind the shock wave E_T equals the initial explosion energy E_0 plus the energy of reaction behind the shock front E_R. For the planar case,

$$E_T = E_0 + E_R = 2\int_0^{r2}\left[\frac{\rho U^2}{2} + \frac{P}{\gamma-1}\right] dr \tag{15a}$$

$$E_R = 2\int_0^{r2} \rho Q\, dr \tag{15b}$$

The self-similar form of E_R is

$$E_R = 2\beta(\gamma+1)E\int_0^1 \frac{g\lambda^{2-n}}{\gamma-k}\, d\lambda \tag{16}$$

The quantity E_R is related to E through another dimensionless coefficient α_R defined by $E_R = \alpha_R E$. Transformation of Eqs. (15) to dimensionless form gives the expression for α:

$$\alpha = \frac{4}{9(\gamma+1)}\int_0^1\left[\frac{gf^2(1+k)^2}{2(\gamma-k)} + \frac{h(1+k)}{\gamma-1}\right] d\lambda - \alpha_R \tag{17}$$

The values of α can be found after integrating Eqs. (10-12).

We have thus reduced the system of partial differential equations (1-3) to the system of ordinary differential equations (10-12), which can be integrated very accurately using standard methods. After finding the values of f, g, h and integrating Eqs. (16) and (17) to find α and α_R, the problem of the strong planar explosion in reactive medium is fully solved. We now show how this solution can be used to solve hypersonic flow problems.

Hypersonic Analogy

The analogy between the problems of strong explosion and steady hypersonic flow was first applied by Lees and Kubota[9] and Grodzovskii.[10] It was also considered in detail by Hayes and Probstein.[5]

Consider hypersonic flow over a thin blunt plate, as shown in Figs. 1a and 1b. According to the hypersonic flow analogy, the hypersonic flow motion over a blunt plate, in the cross sections normal to the direction of U_∞, is similar to the flow due to propagation of a planar point-blast wave. The drag force of the blunt plate is the analog of the point-blast energy E_0.

To apply the solution of the point planar blast in reactive media to steady flows, we use the equivalence principle and replace t by x/U_∞. E_0 can be calculated from

$$E_0 = (1/2)D_f \rho_\infty U_\infty^2 d \tag{18}$$

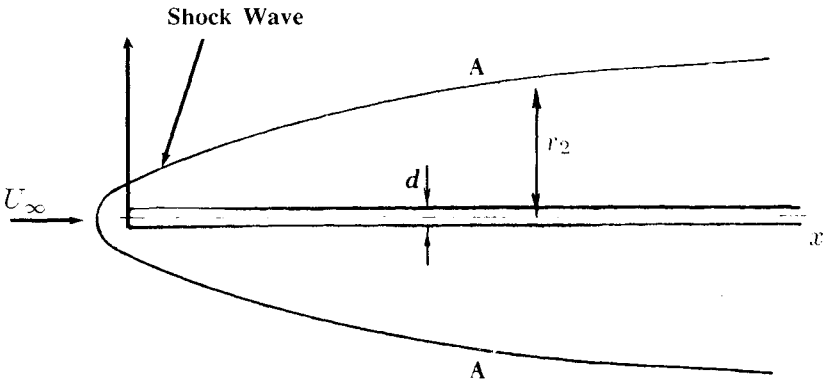

Fig. 1a) Flow over a blunt plate.

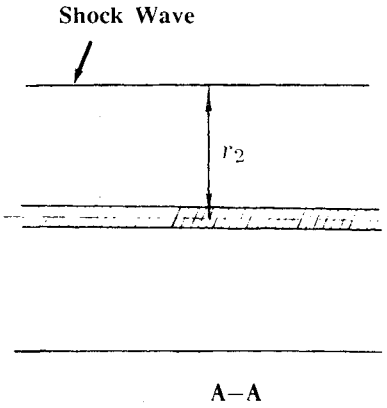

Fig. 1b) Cross section normal to U_∞.

where x is the spatial dimension along the plate as shown in Fig. 1, d the plate thickness, and U_∞ the velocity of the incoming flow. The density of incoming flow is ρ_∞, and D_f is the drag force coefficient.

We make an assumption that the pressure ahead of the shock wave is negligible compared to the pressure behind the wave. We also assume that the flat plate produces a finite amount of drag. Behind the blunted nose, the plate has constant thickness and zero slope.

The function Q, which defines the energy release in reactive media, depends on the new parameters according to

$$Q = \beta\left(\frac{E}{\rho_1}\right)^{n/3}\left(\frac{x}{U_\infty}\right)^{2n/3-2} r^{2-n} \tag{19}$$

In this form, the energy release behind the shock wave is a function of the distance from the nose of the blunt plate x and of the distance from the plane of symmetry r. The main objective of our study is to use the self-similar solutions to validate the numerical solution of reactive hypersonic flows. Several forms of Eq. (19) satisfy that requirement. However, for some values of n the form of Eq. (19) is particularly interesting. For example, when $n = 0$, the energy source term has the form $Q = \text{const} \times (r^2/x^2)$. This form of Q simulates large energy release (or absorption when β is negative) at the nose of the blunt plate and immediately behind the shock front. This could model high-Mach-number flow with substantial ionization at the shock surface and the region of the blunt nose of the plate.

Numerical Simulations

As an example of the application of the self-similar solution for validation of the numerical simulations of hypersonic flow, we present here results of modeling adiabatic hypersonic flow with Mach number $M = 32$ over a thin flat plate. For this test case, the self-similar problem described above reduces to the problem of the classical point blast. The solution for the adiabatic blast is included in Eqs. (4–18) as a special case when $k = 1$ and $\beta = 0$.

The numerical simulations were done using the codes based on the first- and second-order-accurate Godunov method.[11] In Fig. 2, the computational domain and a sample of the grids used for the numerical simulations are shown.

It was assumed that the thin plate is moving with a constant velocity of $U_\infty = 10{,}011$ m/s, parallel to the x axis. This velocity corresponds to the global Mach number of 32 in the ambient air with the parameters corresponding to the standard atmosphere at the altitude of 50 km:

$$P = 98.72 \text{ Pa}, \quad \rho = 1.24 \cdot 10^{-3} \text{ kg/m}^3, \quad \gamma = 1.2, \quad U = 0$$

The thickness d of the flat plate is 0.025 m.

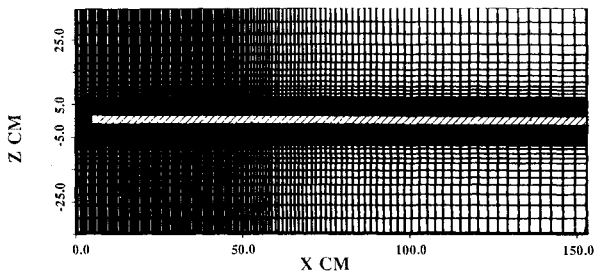

Fig. 2 Computational domain and grid.

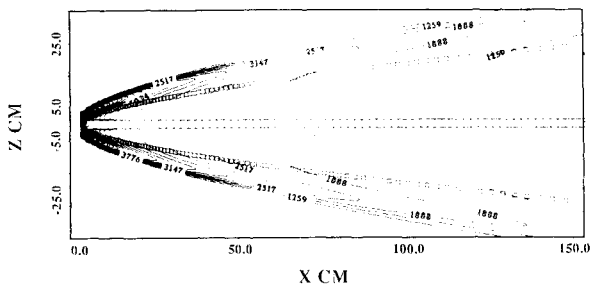

Fig. 3 Pressure contours. First-order Godunov method. Squares indicate shock-front location calculated analytically.

It is assumed that the flow is inviscid and can be described by the following set of two dimensional Euler equations in Cartesian coordinates:

$$\frac{\partial Q}{\partial t} + \frac{\partial F}{\partial x} + \frac{\partial G}{\partial y} = 0 \tag{20}$$

where

$$Q = \begin{bmatrix} \rho \\ \rho u \\ \rho v \\ e \end{bmatrix}, \quad F = \begin{bmatrix} \rho u \\ \rho u^2 + p \\ \rho uv \\ (e+p)u \end{bmatrix}, \quad G = \begin{bmatrix} \rho v \\ \rho vu \\ \rho v^2 + p \\ (e+p)v \end{bmatrix}$$

This system of equations was solved numerically. By time marching, we have obtained steady-state solutions for $t \to +\infty$.

In Fig. 3, we show the results for the simulation obtained using the first-order Godunov method in the form of pressure contours for steady-state solution. This simulation was done on a 100×100 grid, with the sides of the cells at the leading edge twice as long in the x direction as its size in the y direction. Behind the leading edge, the cells were stretched in the x direction as shown in Fig. 2. It is clear from Fig. 3 that the numerical solution exhibits properties characteristic of the very high Mach number hypersonic flows with the shock wave

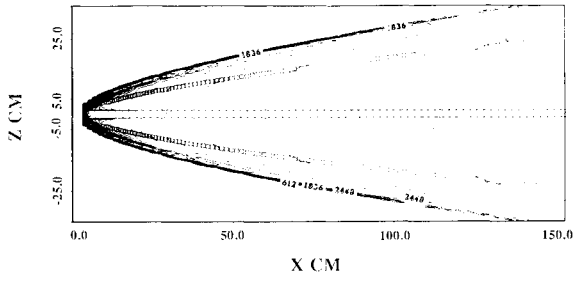

Fig. 4 Pressure contours. Second-order Godunov method. Squares indicate shock-front location calculated analytically.

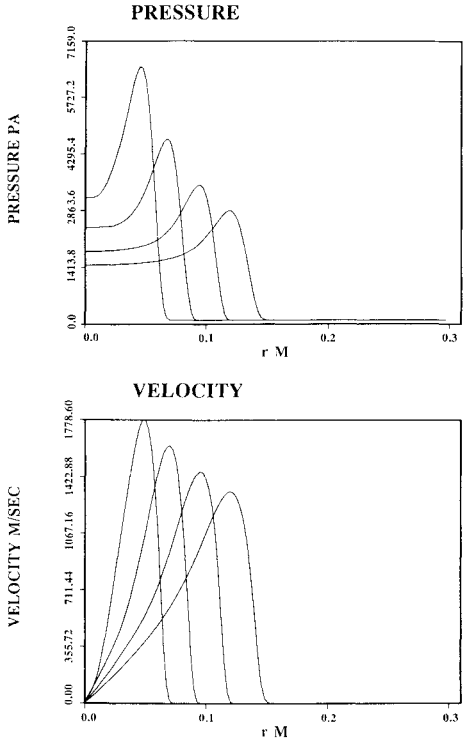

Fig. 5 Distributions of pressure and velocity for vertical cross section of the flow at $x_1 = 0.047$ m, $x_2 = 0.112$ m, $x_3 = 0.245$ m, and $x_4 = 0.438$ m.

at the leading edge repeating the streamlines of the flat plate blunt leading edge. This indicates that flow at this speed approaches that of the Newtonian model.

In Fig. 4, we show results for the same flow conditions as described above obtained on the same grid using the second-order Godunov method. Comparing first- and second-order-accurate solutions, we can notice a substantially sharper shock resolution of the second-order-accurate simulation. However, the locations of the shock waves are the same for both simulations.

Distributions of the pressure and velocity are shown in Fig. 5 for the vertical cross sections of the hypersonic flow at the following distances from the leading edge:

$$x_1 = 0.047 \text{ m}, \quad x_2 = 0.112 \text{ m}, \quad x_3 = 0.245 \text{ m}, \quad x_4 = 0.438 \text{ m}$$

These distributions based on the first-order Godunov results are typical of the point-blast solutions.[5] In Fig. 5, the shock front becomes smeared for the cross sections taken farther downstream, which reflects reduced numerical resolution due to a diverging grid covering computational domain. However, based on the appearance of the solution we can only conclude that it looks qualitatively correct. We will show below how the self-similar solution described above can be used for validation of the numerical results.

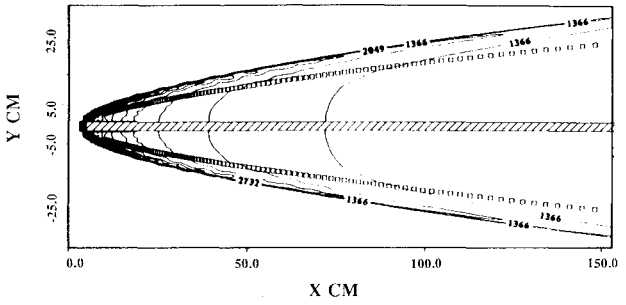

Fig. 6 Pressure contours. Second-order Godunov solution on 150 × 140 grid. Squares indicate shock-front location calculated analytically.

Comparison Between Computation and Theory

We assume that the flow is inviscid, that there is no energy release after the explosion (drag force produced only by the leading edge in the hypersonic flow analogy), and that the ambient pressure is negligible compared to the pressure on the shock wave. Then, the energy released at the blunt leading edge of the flat plate can be calculated using Eq. (18). If we take $D_f = 1$ (the maximum value for inviscid flow), we have $E_0 = 1553$ J/m^2 for the case simulated above. For the adiabatic case from Eq. (8b), we can obtain the following expression relating the shock-front location for fully developed hypersonic flow to the distance from the leading edge and the flat plate thickness:

$$r_2 = \left(\frac{1}{2} D_f \frac{dx^2}{\alpha}\right)^{1/3} \tag{21}$$

where α is defined by Eq. (17) simplified for the adiabatic case by letting $\beta = 0$ and $k = 1$ [from Eq. (13)]. An approximate value for α for $1.2 \le \gamma \le 2$ could be calculated with 0.46% accuracy from the following empirical formula suggested by Korobeinikov[12]:

$$\alpha = k_1(\gamma - 1)^{k_2 + k_3 lg(\gamma - 1)} \tag{22}$$

where $k_1 = 0.36011$, $k_2 = -1.2537$, and $k_3 = -0.18471$. For the adiabatic flow with $\gamma = 1.2$, Eq. (22) gives $\alpha = 2.2$.

In Figs. 3 and 4, the shock-front location (squares) calculated using Eq. (21) is compared with the numerical calculations using the first- and second-order Godunov methods. The numerical simulation predicts a shock front with a significantly larger shock angle. Further comparison shows that in order to match the shock front calculated numerically, the analytical model should have $D_f \approx 3.6$ in Eq. (21). This means that the shock front calculated numerically corresponds to the flat plate with a leading edge about four times large than the real leading-edge thickness in the calculation. Or in other words, the numerical dissipation introduced by the code is four times larger than the invisicid drag produced by the plate leading edge. In these two simulations, the drag predicted by the numerical simulation is about three times larger than the viscous drag obtained in the experiments.[9]

In view of the poor accuracy of the numerical simulation, we decided to simulate the same case on the grid with increased resolution in the direction of the x axis. We developed a 150 × 140 grid, where the grid density in the direction of the x axis was increased twice in the area of the leading edge. We modified the grid density along the y axis only in the area outside the leading-edge region. For this grid, the cell sizes in the x and y directions are equal in the region of the leading edge. Figure 6 shows pressure contours, for the same hypersonic flow problem as above, simulated using the second-order-accurate Godunov method on the new grid. In Fig. 6, the location of the shock front in accordance with the self-similar solution is shown by small squares. Comparing the results in Fig. 6 with the results shown in Fig. 4, we notice a substantial

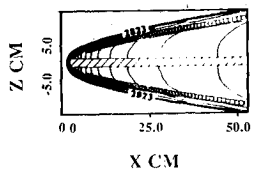

Fig. 7 Pressure contours. Second-order Godunov solution on 300 × 60 grid. Squares indicate shock-front location calculated analytically.

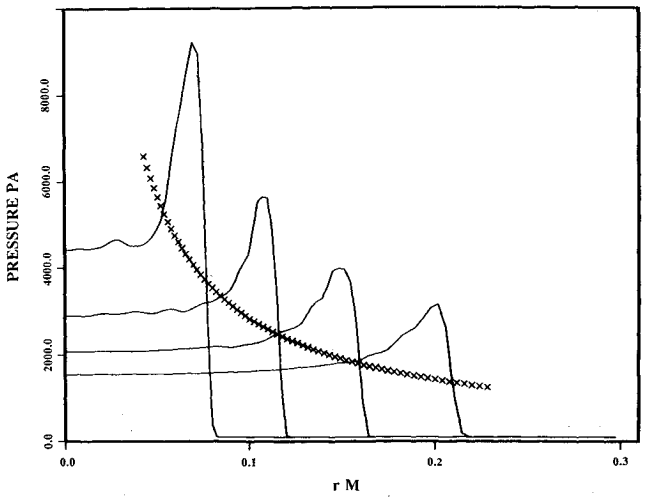

Fig. 8 Pressure distribution in number of vertical cross sections. Second-order-accurate simulation on 100 × 100 grid. ×: shock overpressure calculated analytically.

improvement in the shock location. The shock wave in Fig. 6 is located much closer to the analytical solution. The shock location in this case corresponds to $D_f = 2.4$ in Eq. (21). This means the simulated flow still has a very large drag coefficient, and the shock location corresponds to inviscid flow over a plate twice as thick as the plate we used in the simulation.

To improve the accuracy of the simulation further, we developed a 300 × 60 grid where in the region of the leading edge the grid density in the direction of the x axis was doubled the grid density in the y direction. Near the leading edge, the dimensions of the grid cell in the y direction are the same as in the previous two cases. The results for the simulation on this dense grid are shown in the form of pressure contours in Fig. 7. Here we notice that the numerical simulation converges further to the analytical solution. The very high grid density gives the simulated shock location much closer to the leading edge than in all the previous cases. An estimate of the shock-wave location shows that the numerically simulated flow has an effective drag coefficient $D_f = 1.75$. In the literature,[13] D_f values from 1.2 to 1.75 were used to match the experimental results for hypersonic flow over a flat plate. Even if this value of D_f approaches the experimentally measured drag for a thin blunt plate, it is still very high for inviscid calculation.

Using Eq. (4), (9), and (18), it is possible to calculate the value of the pressure at the front of the shock wave:

$$P_2 = (8/9) \times [E/(\gamma + 1)r_2] \tag{23}$$

where r_2 is calculated from Eq. (21) and E could be calculated from $E_0 = \alpha E$ for an adiabatic case. For the case of the hypersonic flow over a blunt flat plate, considered above, we have $E = 706\ \mathrm{Jm}^{-2}$.

Figure 8 shows the pressure distribution in several vertical cross sections of the flow as a function of the distance from the flat plate surface calculated using the second-order-accurate simulation on the coarse grid. (The pressure contours for this simulation are shown in Fig. 4.) The values of maximum overpressure calculated analytically using Eq. (23) are indicated by the symbol ×. The first cross from the left corresponds to the first cross section from the left of the numerical solution shown on the same figure. From that point on, we have calculated P_2 for every cross section corresponding to the grid points on the x axis. The analytical curve is shifted to the left since the angle of the analytically predicted shock is substantially smaller. Although the pressure distribution behind the shock wave is very similar to the pressure distribution for the blast wave, the pressure values for the numerical simulation are substantially larger ($\approx 40\%$). This can be explained by the larger effective drag simulated numerically.

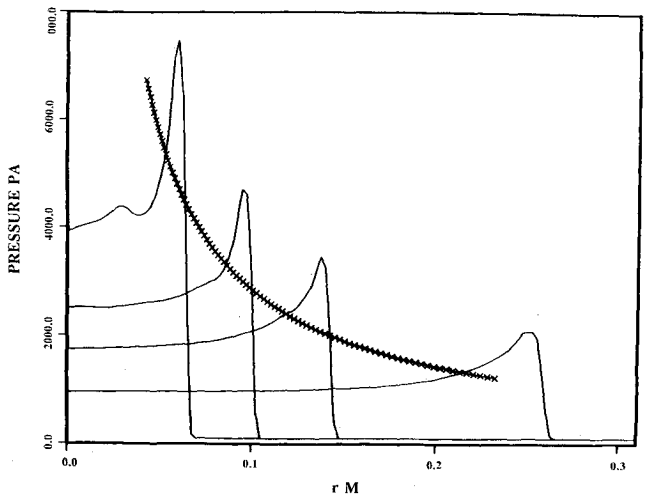

Fig. 9 Pressure distribution in number of vertical cross sections. Second-order-accurate simulation on 150 × 140 grid. ×: shock overpressure calculated analytically.

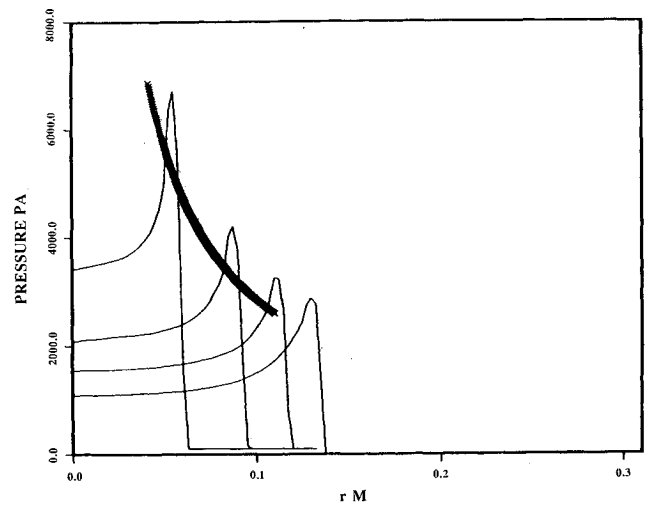

Fig. 10 Pressure distribution in number of vertical cross sections. Second-order-accurate simulation on 300 × 60 grid. ×: shock overpressure calculated analytically.

Figures 9 and 10 show numerical and analytical shock-waves pressures in the same format as in Fig. 8 for the simulations on the 150 × 140 and 300 × 60 grids, respectively. It is clear from these figures that the numerical solution converges to the analytical solution with increase of the grid resolution in the x direction. For the simulation on 300 × 60 grid, the difference between maximum pressures calculated analytically and numerically is less than 5%. It is also interesting to observe that in this case the analytical value is slightly higher, which may reflect insufficient grid resolution to pick up the highest pressure at the shock front.

Conclusions

We have developed a family of self-similar solutions for hypersonic flow over a flat plate with a blunt leading edge.

These solutions include simulation of the energy release (or absorption) behind the main shock front and are derived based on the principle of hypersonic similitude from the solutions of the point-blast problem with energy release. The form of the energy release function $Q(x,r)$ allows simulation of the effects of the variety of the model heat-release functions in the hypersonic flow.

The resulting solution presents a particular interest as a test problem for numerical simulations of hypersonic flows. We have demonstrated an example of this application for hypersonic flow with $M = 32$ over a flat plate 0.025 m thick. Numerical simulations were done using the Godunov method and its second-order extension on a succession of grids covering the computational domain with increased density. As a result of comparison between the numerical solution and the solution of the self-similar problem, we can conclude that the numerical solutions converging to the analytic solution with increase of grid density in the direction of the main velocity vector. The numerical solutions display a strong dependence on the grid density and structure, and even for the densest grid used in the simulations the amount of diffusion was above the level expected for the viscous flow regime. The differences between the analytic and numerical solutions are apparent in both shock location and overpressure levels. For some calculations presented here, the numerical simulation gives a shock location corresponding to the plate about four times thicker than actually used in the simulations.

This example of the application of the analytical solution illustrates its importance for validation of the numerical solution. Without having the reference point, it would have been very difficult to evaluate how accurate the numerical solution is and the solution on the coarser grid with an erroneous shock angle could be judged as adequate. An additional benefit of using the analytical solution of the same mathematical model for validation is the prospect of evaluating the accuracy of the numerical simulation of the mathematical model only without the uncertainties arising from the validation based on experimental data. This can allow a deeper understanding of the sources and nature of numerical errors as well as limitations imposed by these errors. For example, in the case in which we have simulated, the numerical simulation of the inviscid model produces more numerical dissipation than is expected from the natural viscosity. This means, at least on the grids which we have used, that extension of the mathematical model to the Navier-Stokes equations will be pointless without substantial improvement of the solution accuracy.

Application of the self-similar solution with heat release presented here will be especially interesting for validation of the numerical codes which model very complex physical and chemical phenomenon, where knowledge of numerical limitations can substantially simplify the model and help to understand the results.

References

[1]Klopfer, G. H. and McRae, D. S., "Nonlinear Truncation Error of Finite-Difference Schemes for the Euler Equations," *AIAA Journal*, Vol. 21, April 1983.

[2]Mehta, U., Chang, K. C., and Cebeci, T., "Relative Advantages of Thin-Layer Navier–Stokes and Interactive Boundary-Layer Procedures," NASA TM 86778, Nov. 1985.

[3]Fujii, K. and Obayashi, S., "Evaluation of Euler and Navier-Stokes Solutions for Leading-Edge and Shock-Induced Separations," AIAA Paper 85-1563, 1985.

[4]Muller, B., "Navier-Stokes Solutions for Hypersonic Flow Over an Indented Nosetip," AIAA 7th Computational Fluid Dynamics Conference, Cincinnati, OH, July 1985.

[5]Hayes, W. D. and Probstein, R. F., *Hypersonic Flow Theory*, Academic, New York, 1966.

[6]Chernyi, G. G., *Introduction to Hypersonic Flow*, Academic, New York, 1961.

[7]Eidelman, S., Timnat, Y., and Burcat, A., "The Problem of Strong Point Explosion in a Combustible Medium," 6th Symposium on Detonation, Coronado, CA, 1976.

[8]Burcat, A., Eidelman, S., and Timnat, Y., "The Evolution of a Shock Wave Generated by a Point Explosion in a Combustible Medium," Symposium of High Dynamic Pressure, Paris, France, Aug. 1978.

[9]Lees, L. and Kubota, T., "Inviscid Hypersonic Flow Over a Blunt-Nosed Slender Bodies," *Journal of Aeronautical Sciences*, Vol. 24, 1957, pp. 195–202.

[10]Grodzovskii, G. L., "Certain Peculiarities of the Flow Around Bodies at High Supersonic Velocities," *Izvestiya Akademii Nauk SSSR*, Vol. 6, 1957, pp. 86–92.

[11]Eidelman, S., Colella, P., and Shreeve, R. P., "Application of the Godunov Method and Its Second-Order Extension to Cascade Flow Modeling," *AIAA Journal*, Vol. 22, Nov. 1984.

[12]Korobeinikov, V. P., *Problems of the Point-Blast Theory in Gases*, Nauka, Moscow, 1973.

[13]Cheng, H. K. and Pellons, A. G., "Inviscid Leading-Edge Effects in Hypersonic Flow," *Journal of Aeronautical Science*, Vol. 23, 1956.